Extraction of Sea Surface Current Pattern in Bab Al-Mandab Strait using Radar Sentinel-1 C-band SAR Image

Abstract

This paper presents the results of sea surface current pattern (velocity and direction) extraction in Bab Al-Mandab Strait in the south east part of Yemen. The Sentinel-1 (S-1) C-band Synthetic Aperture Radar (SAR) image used in this study is Level-1 (IW) Ground Range Detected (GRD) single mode product. It was acquired on September 8th 2016 at 21:25:12 in VV polarization. The pixel spacing for both range and azimuth is 10 m. The incidence angles ranged between 30.86° at the near range to 36.59° at the far range. Four experimental areas were randomly selected to validate modeled results of the sea surface current patterns extracted from the Sentinel-1 SAR image. The length of each subset image is (512 X 512) pixels across the range resolution. Three different steps were used in this study to extract sea surface current patterns in the study area. The first step is the extraction of distribution of radar cross section. The second step is the calculation of Doppler frequency shift in order to extract the SAR spectra. The final step is to find the sea surface current rose diagram to verify the speed and direction. This study emphasizes the importance of the Doppler frequency by which to extract the sea surface current patterns from SAR images.

Keywords: Bab Al-Mandab Strait, sea surface current pattern, Sentinel-1 (SAR), Doppler frequency

Introduction

Ocean currents influence global and local climates and impact marine life through the redistribution of heat, nutrients, and pollutants. Many of these processes are influenced by the strong current gradients that exist near the boundaries of major current systems and in regions of outflow from rivers and estuaries (Lyzenga et al., 2004, p:210). Researchers have shown increased interest in ocean studies using remote sensing technologies which can image large ocean area and provide precise information on surface ocean dynamics (Wittgenstein, 1992, p:162).

ISSN:2707-8655
EISSN:2707-8663

Spaceborne Synthetic Aperture Radar (SAR) is an active microwave remote sensing instrument providing two-dimensional (2D) information of the normalized radar cross section σ_0 (NRCS), which represents the ability of a surface to reflect the radar signal (Pleskachevsky et al., 2019, p:4116). The results obtained from many application-oriented studies and from the operational use of airborne imaging radars are encouraging (Lee & Kwag, 2005, p:4054). Although remote sensing technology is currently well developed, the investigation of ocean surface current using Synthetic Aperture Radar (SAR) has not been easy (Kim et al., 2004, p:3119). The velocity and the direction of sea surface currents provide scientists a great deal of knowledge on phenomena interchanges on the surface of the ocean.

SAR sensors register microwave radar backscatters which are dependent on patterns of surface roughness in practically all weather conditions (Robinson, 2000, p:323). The interaction between the SAR pulse of microwave energy and the ocean surface is complex, depending on wavelength, polarization, geometry, environmental conditions and the electrical properties of the ocean surface (Holt, 2004, p:50). Actually, these physical complexities make it very difficult to extract the sea surface current patterns (velocity and direction) directly from the SAR imageries. Considerable efforts have been devoted during the past years to improve understanding of the sea surface current patterns through the use of SAR images (Gelpi & Norris, 2003, p:107).

Doppler Frequency Shift

The Doppler centroid anomaly recorded over ocean with a Synthetic Aperture Radar (SAR) can be used to obtain range directed velocity which has been demonstrated to provide valuable estimates of the near surface wind speed, ocean surface current (Harald et al, 2016 p:3994). According to (Kang, 2018, p:6) Doppler parameter from SAR (Synthetic Aperture Radar) is among the most effective tools for velocity measurements. The physical principle for estimating radial velocity utilizes the Doppler shift extracted from SAR data. The Doppler shift is caused by the relative motion between a sensor and target.

(Kim et al., 2004, p:3119) extracted the ocean current based on the concept in which Doppler frequency shift and the ocean current are closely related. Moving targets cause Doppler frequency shift of the backscattered radar radiation of SAR, thus the line-of-sight velocity of the scatters can be evaluated. The Doppler frequency shift can be measured by estimating the difference between Doppler centroid obtained and reference Doppler centroid calculated. (Romeiser et al.2010,

p:82) mentioned that despite the fact that a SAR is a Doppler radar, conventional SAR images do not provide direct information on target velocities, since all Doppler information is normally utilized to obtain the best possible spatial resolution in flight (azimuth) direction.

Sentinel-1 (S-1) C-band

The Sentinel-1 (S-1) C-band Synthetic Aperture Radar (SAR) contributes mainly to the physical oceanography research of sea state, wind sea surface measurements and ocean circulation "surface current" (Malenovsky et al, 2012 p:92).

Sentinel-1 operates at C-band with a nominal frequency range, from 8 to 4 GHz (3.75 to 7.5 cm wavelength). Sentinel-1 data products acquired in four modes which are the Strip Map (SM), Interferometric Wide swath (IW), Extra Wide swath (EW) and Wave (WV) modes (Bourbigot et al, 2016 p:7-9). Extended Wide swath EW and Interferometric Wide swath IW are mainly used for monitoring of sea ice areas and coastal regions over the ocean (Wang et al, 2019 p:106).

Materials and Study Area

The Sentinel-1 image used in this study is Level-1 (IW) Ground Range Detected (GRD) single mode product. It was acquired on September 8th 2016 at 21:25:12 in VV polarization. The pixel spacing for both range and azimuth is 10 m. The incidence angles ranged between 30.86° at the near range to 36.59° at the far range (Table 1).

The study area is located in Bab Al-Mandab Strait in the south east part of Yemen (Figure 1). The study area lies between latitudes 11°59'19"N and 14°10'46"N and longitudes 41°49'44"E and 44°27'36"E (Figure 1).

مجلة المهرة للعلوم الإنسانية
مجلة علمية محكّمة نصف سنوية
العدد العاشر- شوال/ذي القعدة ١٤٤٢هـ يونيو ٢٠٢١م
ISSN:2707-8655
EISSN:2707-8663

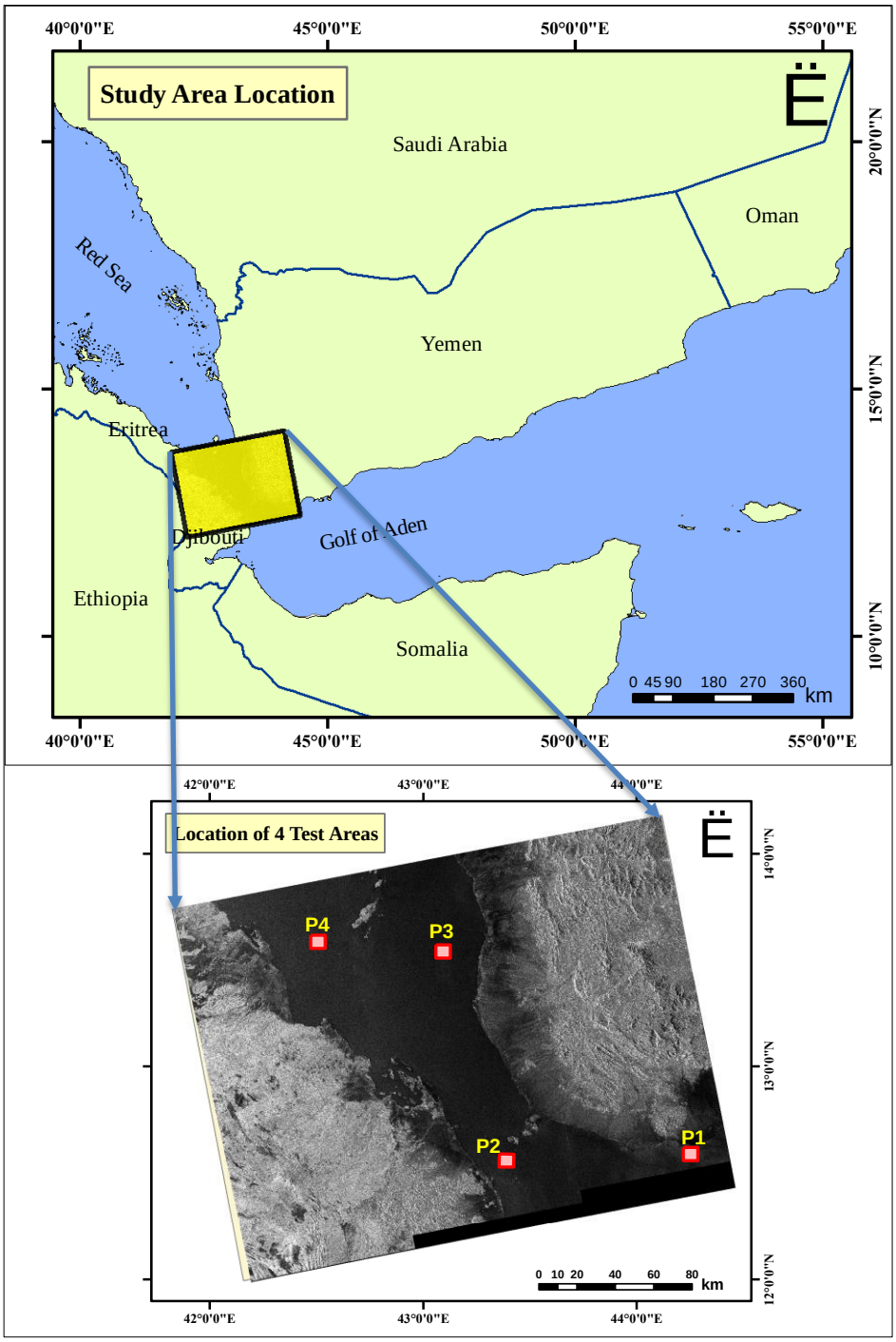

Figure 1. Locations of Study area and the four experimental areas

Table 1. Sentinel-1 C-band SAR Image Description

Start time	Beam	Polarization	Pixel Spacing Rng x Azi (m)	Incidence Angle (deg)	Swath width (km)
08/09/2016 21:25:12	S1A_IW_GRDH-HR	VV	10x10	30.86-36.59	250

Experimental Areas

Four experimental areas were randomly selected to validate modeled results of the sea surface current patterns extracted from the Sentinel-1 SAR image. The length of each subset image is (512 X 512) pixels across the range resolution (Figure 1).

Method and Results

Three different steps were used in this study to extract sea surface current patterns in the study area. The first step is the extraction of distribution of radar cross section. The second step is the calculation of Doppler frequency shift in order to extract the SAR spectra. The final step is to find the sea surface current rose diagram to verify the speed and direction.

Distribution of Normalized Radar Cross Section

The normalized radar cross section (NRCS) σ_0 is the common radar parameter used to describe radar return backscattered by the ocean surface to the SAR sensors. NRCS was computed using equation (1) as shown by (Wang et al, 2019 p:107).

$$\sigma_0 = \frac{|DN|^2}{SigmaNaught^2} \qquad (1)$$

The distribution of the radar cross section of four experimental areas which extracted from Sentinel-1 C-band mode is illustrated (Figure 2). Comparing them, one can estimate the distribution and difference of the backscatter values. The radar cross section values extracted from area (1) in the onshore ranges between -4 to -16 dB. However, radar cross section values increased in area (2) which is located in Bab Al-Mandab and ranges between -4 to -24 dB. This is due to the increased speed

ISSN:2707-8655
EISSN:2707-8663
مجلة علمية محكّمة نصف سنوية
العدد العاشر- شوال/ذي القعدة ١٤٤٢هـ يونيو ٢٠٢١م

and turbulence of sea currents as they enter the Bab al-Mandab Strait, south of the Red Sea. In comparison, the radar cross section value in the offshore is high and equal in both areas (3) and (4) and ranges from -4 to -24 dB. EH6 mode cross section value in the on shore ranges from -18 to -27 dB. Another important finding is the result of the radar cross section in the onshore and offshore is the sea surface roughness. It is clear that the backscatter values of radar image reflect the roughness of the sea surface in the onshore which is lower compared to those of the offshore.

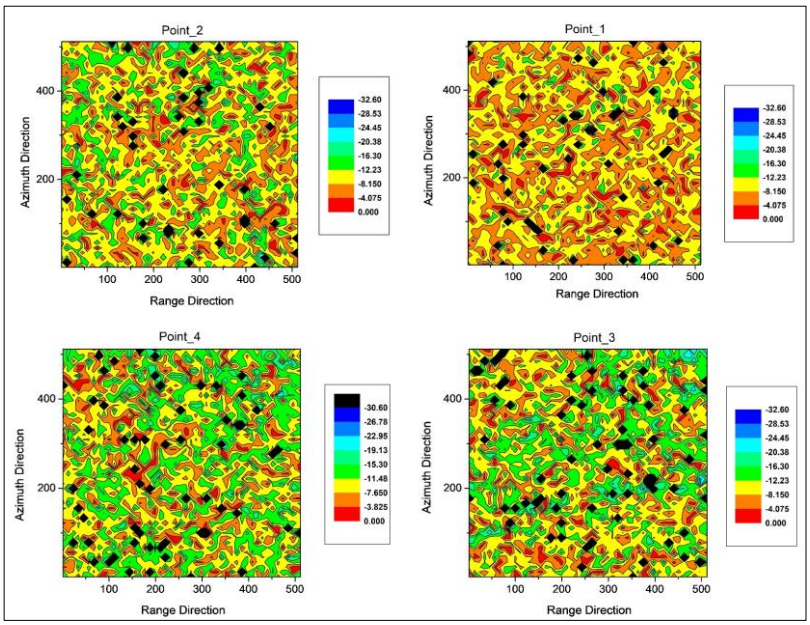

Figure (2): Distribution of radar cross section in the four experimental areas

Doppler Frequency Shift Spectra

SAR utilizes the Doppler shift of the complex receiving field to locate scatterers in the flight direction. This complex field and its associated residual Doppler shift can be used to infer the velocity of these scatterers as reflected by ocean currents (Hasselman, 1980, p:228). The selected four areas consist of several adjoining pixels and it must have the highest signal amplitude than the surrounding pixels. The Doppler spectrum of range compressed Sentinel-1 SAR image was estimated by performing a Fast Fourier Transform (FFT) and Inverse Fast Fourier Transform (IFFT) as given in equation (2).

$$F(u)=\int_{-\infty}^{\infty} f(x)e^{-2\pi iux}dx \qquad 2)$$

where $F(u)$ is a frequency domain function, u is the spatial frequency, and $f(x)$ is the spatial domain function. The spectral density is a response from infinitesimal point scatterers. A closed form solution can be given for the Doppler spectral density as in the expression (3) (Hasselman, 1980, p:228):

$$G(x_0,\omega)=H(\omega)e^{i\omega' x_0/V}\int_{-\infty}^{\infty}\exp\left[-\frac{2}{T_s{}^2}\left(1+\left(\frac{T_s}{T}\right)^2-\frac{ibT_s{}^2}{4}\right)\tau^2-\frac{4}{T_s}\left(\frac{x_0}{VT_s}+i\frac{\omega' T_s}{4}\right)\tau-\frac{2x_0{}^2}{V^2T_s{}^2}\right]d\tau \qquad 3)$$

where x_0 is the location of a point target in the SAR image, T_s is the Gaussian function with width, V is the satellite velocity (6761m/s), τ is the delay time = $t-x_0/V$ and $x_0=vt$, and b is the chirp rate = $2kv^2/R$. Equation (3) was used to determine the spectral magnitude. Image intensity is related to spectral magnitude in finding out the radial current velocity.

The spectra of Doppler frequency shift of four selected areas used to simulate the sea surface current patterns from Sentinel-1 C-band mode is shown in (Figure 3). The results of spectra in all areas were ranged between (-0.002db) to (0.012db). The spectra peak of area 1 was (0.012db) and shows strong shift towards the azimuth direction. This related to the strong current occurrence which leads to strong nonlinearity as compared to the other areas. The spectra peak of area 3 was (0.010db) and shows medium shift, while spectra peak of areas 2 and 3 were (0.008db) and show small shift towards the azimuth direction. In addition, the spectra peak of Doppler in all areas were shifted towards the azimuth direction due to the effect of the nonlinearity between SAR pulse and sea surface current movements. This result agrees with previous studies of (Gonzalez, et all. 1981) and (Chapron, et all. 2005, C07008.11).

Surface current rose diagram

The rose diagram of the sea surface current patterns was extracted from the experimental areas. The mean value of surface current speed and directions vary in all areas as shown in Figure (4). The mean value of speed in area (1) was 0.9 m/s,

ISSN:2707-8655
EISSN:2707-8663
مجلة المهرة للعلوم الإنسانية
مجلة علمية محكّمة نصف سنوية
العدد العاشر- شوال/ذي القعدة ١٤٤٢هـ يونيو ٢٠٢١م

and the currents flow southwestward azimuth direction (62.1^0). The mean value of speed in area (2) in Bab Al-Mandab was 1.1 m/s, and the currents flow northward and northwestward azimuth direction ($162\ ^0$). The mean value of speed in area (3) was 1.1 m/s, and the currents flow northwestward azimuth direction (145^0). The mean value of speed in area (4) was 1.2 m/s, and the currents flow westward azimuth direction (107.6^0). It is clear that the sea surface pattern speed increased in Bab Al-Mandab and south of the Red Sea.

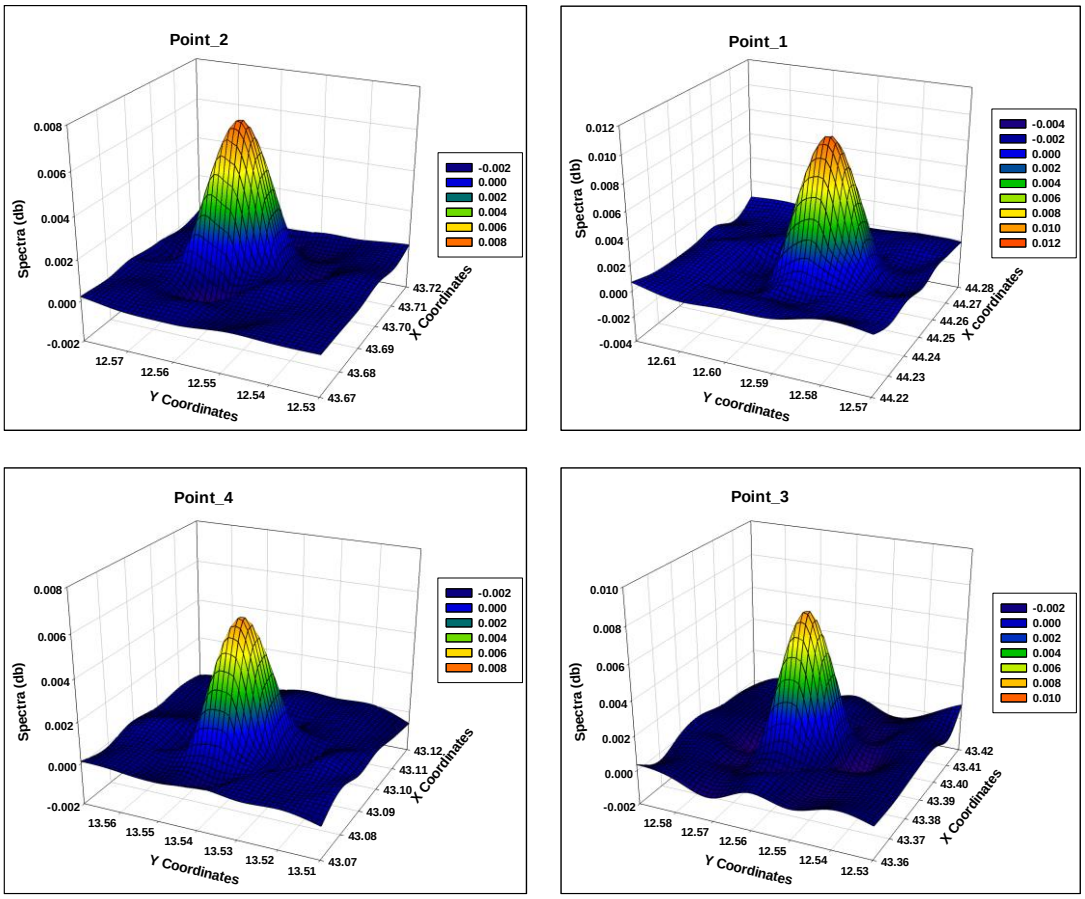

Figure3: Doppler frequency shift spectra of Sentinel-1 C-band mode extracted from the experimental areas

Sea Surface Current Patterns

The RADARSAT-1 SAR ocean current values have been converted to the horizontal ocean current V_c on the ocean surface. The radial component of ocean current deduced from RADARSAT-1 SAR images is given in terms of the Doppler

peak frequency shift, $f_{\max}$ therefore the horizontal ocean current is computed by using equation (4), (Johannessen, et al., 2006, p:77).

$$V_c = \frac{2}{N}\left[\frac{\lambda V\left(1+\Delta f_a / \Delta f_h\right)^2}{2\rho_a \sin\theta \sin\Phi}\right]\left(\Delta f_a\right)^{-1} \tag{4}$$

Due to the imaging nature of the SAR, the direction of the sea surface current in the range direction is impossible to find. However, the equation (5) introduced by (Maged, 2005, p:148) was used to determine the current in the azimuth direction.

$$\theta = \tan^{-1}\frac{\left(\lambda f_D\right)\left(2\sin\theta\right)^{-1}}{V\left(1-\left(1-2\Delta x \partial x v_s\right)^{-0.5}\left(\Delta f_D R\lambda\right)\right)^{-1}} \tag{5}$$

where V is the satellite velocity, R is the slant range, Δ_x is the displacement vector and ∂_x is the pixel spacing in the azimuth direction.

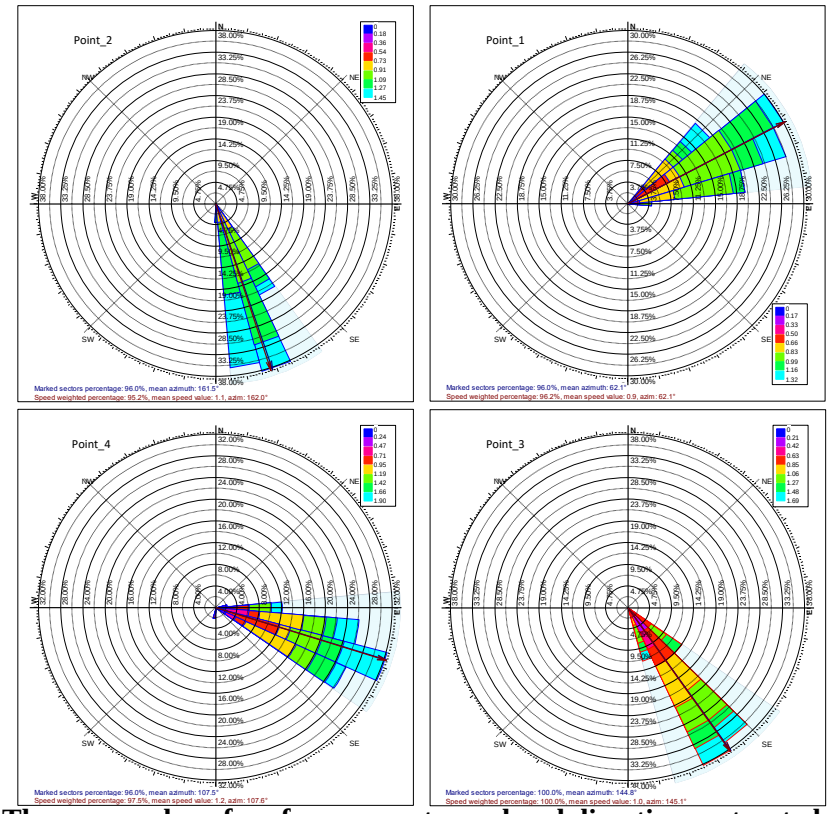

Figure (4): The mean value of surface current speed and directions extracted

ISSN:2707-8655
EISSN:2707-8663
مجلة المهرة للعلوم الإنسانية
مجلة علمية محكّمة نصف سنوية
العدد العاشر- شوال/ذي القعدة ١٤٤٢هـ يونيو ٢٠٢١م

from the experimental areas

The sea surface current patterns (velocity and direction) extracted from Sentinel-1 (S-1) C-band mode is shown in Figure 5. It is clear that the sea surface current direction was westward in Gulf of Aden to the north and north-westward in Bab Al-Mandab and the Red Sea. The vector plotted on the image shows that the sea surface current velocity in Gulf of Aden was averaged between 0.81m/s to 0.95 m/s near the offshore area. The sea surface current velocity in Bab Al-Mandab increased to become around 1.10 m/s. it is obviously that the sea surface current velocity in the Red Sea increased to around 1.23 m/s in the mid-shore and onshore.

The surface current direction mostly was westward in the study area including the onshore. The surface current velocity was generally regular in the study area except in the onshore area where the grid vectors show that the current velocity slightly increased. The current direction is related to the information of the current velocity. This information has a strong relation with the image backscatter and the Doppler frequency values.

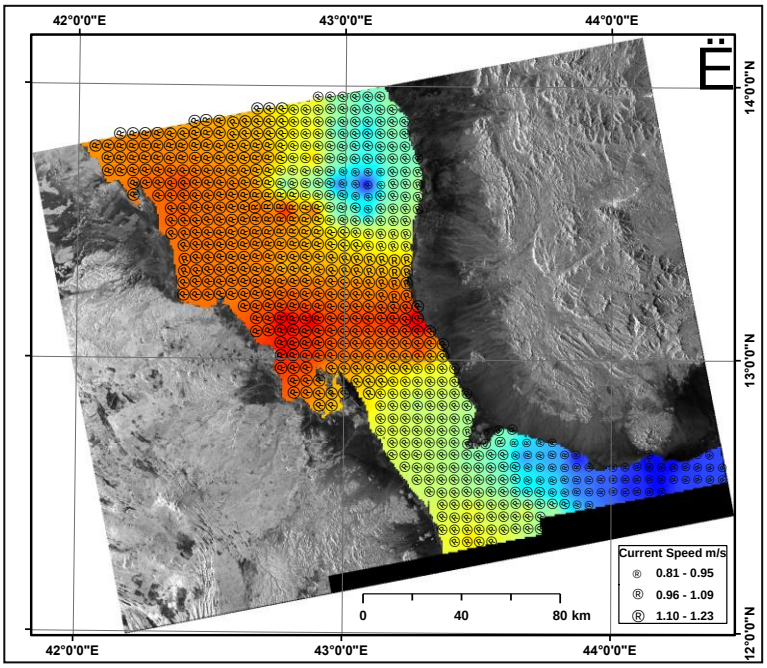

Figure (5): Sea surface current patterns extracted from Sentinel-1 (S-1) C-band

Conclusion

This study emphasizes the importance of the Doppler frequency by which to extract the sea surface current patterns from SAR images. It is interesting to note that along the study area from the coastline to the sea, the increase in the radar cross section values is accompanied with corresponding increase in the Doppler shift frequency too. This reflects the fact that Doppler frequency is dependent on the backscatter values of the radar image. This result is consistent with (Romeiser, 1994, p:730) who suggested that Doppler shift of the backscattered radar signal from the sea surface can be used for determining the line-of-sight velocity of the scatterers and thus for measuring surface current and ocean wave spectra.

References

1. Bourbigot, M.; Johnsen, H.; Piantanida, R. (2016) "Sentinel-1 Product Definition" Chapron, B.; Collard, F.; Ardhum, F. Direct Measurements of Ocean Surface Velocity from Space: Interpretation and Validation. *Journal of Geophysical Research*. 2005, 110, C07008.1-C07008.17.
2. Gelpi, C. G.; Norris, K. E. Estimated Surface-Wave Contributions to Radar Doppler Velocity Measurements of the Ocean Surface. *Remote Sensing of Environment Journal*. 2003, 87, 99-110.
3. Gonzalez, F. I.; Rufenach, C. L.; Shuchman, R. A. Ocean Surface Current Detection by Synthetic Aperture Radar. Proceeding of the COSPAR/SCOR/IUCRM *symposium on oceanography from space*. NY. 1981, 511-523.
4. Harald, J.; Vegard, N.; Geir, E.; Alexis, M.; Fabrice, C. 2016 "Ocean doppler anomaly and ocean surface current from Sentinel 1 tops mode" *Geoscience and Remote Sensing Symposium* (IGARSS), 2016 IEEE International. 10-15 July 2016, Pages 3993-3996

ISSN:2707-8655
EISSN:2707-8663

5. Hasselman, K. A, Simple Algorithm for the Direct Extraction of the Two Dimensional Surface Image Spectrum from the Return Signal of Synthetic Aperture Radar. *International Journal of. Remote Sensin*g 1980, 1, 219-240.

6. Holt, B. SAR Imaging of the Ocean Surface. Synthetic Aperture Radar Marine's User Manual book. USA, Department of Commerce, Washington, DC; September, 2004; Chapter 2, pp 48-51.

7. Johannessen, J. A.; Kudryavtsev, V.; Chapron, B.; Collard, F.; Akimov, D.; Dagestad, K. F. Backscatter and Doppler Signals of Surface Current in SAR Images: A Step towards Inverse Modeling. SEASAR 2006 *Advances in SAR Oceanography from Envisat and ERS*. Missions 2006.

8. Kang, K. (2018) Doppler parameter estimation from SAR (Synthetic Aperture Radar) for velocity measurements: Sea surface current and ship velocity. Phd Thesis, School of Earth and Environmental Sciences, Seoul National University, pages 134

9. Kim, J. E.; Kim, D.; Moon, W. M. (2004) "Enhancement of Doppler Centroid for Ocean Surface Current Retrieval from ERS-1/2 Raw SAR". *IEEE International Geoscience Remote Sensing Symposium*. 5, 3118-3120

10. Lee, W. K.; Kwag, Y. K. (2005) "SAR System Technology Development for Korean Peninsula". *IEEE International Geoscience Remote Sensing Symposium*. 6, 4053-4056.

11. Lyzenga, D. R.; Marmorino, George. O.; Johannessen, J. A. (2004) "Ocean Currents and Current Gradients". NOAA SAR Manual Chapter (8), *National Oceanic and Atmospheric Administration*, Washington, 207-220.

12. Maged, M. M. Modeling of Current Velocities from Advection Process along Kuala Terengganu Coastal Waters. *Asian Journal of Information Technology*. 2005, 4, 147-151.

13. Malenovsky, Z.; Rott, H.; Cihlar, J.; Schaepman, M, E.; GarcíaSantos, G.; Fernandes, R.; Berger, M. (2012) " Sentinels for science: Potential of Sentinel-1, -2, and -3 missions for scientific observations of ocean, cryosphere, and land" *Journal of Remote Sensing of Environment*. 120 (2012) 91–101

14. Pleskachevsky, A.; Jacobsen, S.; Tings, B.; Schwarz, E. "Estimation of sea state from Sentinel-1 Synthetic aperture radar imagery for maritime situation awareness" *International Journal of Remote Sensing* 2019, Vol. 40, No. 11, 4104–4142

15. Robinson, I. S. Space Techniques for Remote Sensing of Environmental Risks in Seas and Oceans. *Journal of Surveys Geophysics*, 2000, 21, 317-328.

16. Romeiser, R. Doppler Spectra of the Radar Backscatter from the Sea Surface Obtained from A Three-Scale Composite Surface Model. IEEE International *Geoscience Remote Sensing Symposium* 1994, 2, 729-731.

17. Romeiser, R.; Johannessen, J.; Chapron, B.; Collard, F.; Kudryavtsev, V.; Runge, H. (2010) Direct Surface Current Field Imaging from Space by Along-Track InSAR and Conventional SAR. *Oceanography from Space Book*, Springer, pp 73-91

18. Wang, C.; Mouche, A.; Tandeo, P,; Stopa, J. E.; Longepe, N.; Erhard, G.; Foster, R, C.; Vandemark, D.; Chapron, B. (2019) "A labelled ocean SAR imagery dataset of ten geophysical phenomena from Sentinel-1 wave mode" *Geoscience Data Journal*. 2019; 6:105–115 DOI: 10.1002/gdj3.73

19. Wittgenstein, S. L. (1992) "Barriers to the Use of Remote Sensing in Providing Environmental Information". *Journal of Environment Monitor Assessment*. 20, 159-166.

مجلة المهرة للعلوم الإنسانية
مجلة علمية محكّمة نصف سنوية
العدد العاشر- شوال/ذي القعدة ١٤٤٢هـ يونيو ٢٠٢١م
ISSN:2707-8655
EISSN:2707-8663

ملخص

استخراج أنماط تيارات سطح البحر في مضيق باب المندب باستخدام مرئية الرادار Sentinel-1 C-band SAR

أ.م.د. محمد أحمد مياس[1]

ملخص البحث:

يعرض هذا البحث نتائج استخراج نمط تيارات سطح البحر (السرعة والاتجاه) في مضيق باب المندب في الجزء الجنوبي الشرقي من اليمن باستخدام مرئيات رادار Sentinel-1 SAR التي تم تصويرها في 8 سبتمبر 2016 الساعة 21:25:12 باستقطاب VV، وبمقدار 10م لتباعد البكسل في كل من اتجاه المدى والسمت، وتراوحت زوايا السقوط بين 30.86(في المدى القريب و 36.59) في المدى البعيد، وقد تم اختيار أربع مناطق تجريبية بشكل عشوائي للتحقق من صحة النتائج النموذجية لأنماط تيارات سطح البحر المستخرجة من مرئية SAR، ويبلغ طول كل صورة مجموعة فرعية (512 × 512) بكسل، كما تم استخدام ثلاث خطوات مختلفة في هذه الدراسة لاستخراج أنماط تيارات سطح البحر في منطقة الدراسة، وكانت الخطوة الأولى: عن طريق استخراج توزيع المقطع العرضي للرادار، والخطوة الثانية: هي حساب إزاحة تردد دوبلر (Doppler Frequency) لاستخراج الأطياف، والخطوة الأخيرة: هي الحصول على رسم تخطيطي لتيار سطح البحر للتحقق من السرعة والاتجاه، وتؤكد هذه الدراسة على أهمية تردد دوبلر لاستخراج أنماط تيارات سطح البحر من مرئيات Sentinel-1.

الكلمات المفتاحية: مضيق باب المندب، نمط تيارات سطح البحر، Sentinel-1 SAR، تردد دوبلر.

(1) أستاذ مشارك، وحدة المعلومات الجغرافية، قسم الجغرافيا والجيوانفورماتكس، كلية الآداب والعلوم الإنسانية، جامعة صنعاء.